Development and Validation of Nonlinear Dynamic Analysis in Seismic Performance Verification of Underground RC Structures

Jun Matsui[1], Keizo Ohtomo[2] and Kensei Kanaya[3]

Abstract

Large shake table test and subsequent numerical analysis correlation were conducted to develop and validate a suitable nonlinear FEM model for the seismic performance evaluation of underground RC structures, enhancing the existing skeleton and hysteresis rules for RC members. A trilinear nonlinear RC member model that represents the effect of reinforcing bar pullout was developed and validated through numerical correlation analysis using past static loading tests. The shake table test results demonstrate that the deformation of model RC structure is fully governed by ground deformation both in the elastic and inelastic ranges. The FEM model developed here derives estimations that show good correlation with test results in terms of such parameters as structural deformation, shear stress distribution on the upper slab surface and concrete cracks and reinforcing bars yielding events, because of the successful parameter identification of nonlinear soil and RC member models.

1. Introduction

With regard to the establishment of seismic performance verification for reinforced concrete (hereafter, RC), underground structures have become the focus of much attention in earthquake engineering circles since the devastating damage to subway tunnels (Iida et al. 1996) inflicted by the 1995 Hyogoken Nanbu Earthquake. The most important lesson learned from the damage caused by this earthquake is that structural collapse should at least be avoided during severe ground motion regardless of whether it leaves some extent of transverse residual deformation or not. Observation of the impact of this earthquake also suggests that it is essential to consider adequate soil-structure interaction effect associated with the nonlinearity of soil and structure in analysis models for seismic performance evaluation when focusing on structural deformation. In this context, the finite element method (hereafter, FEM) has a great advantage for representing dynamic and nonlinear soil-structure interaction, although it sometimes requires heavy computational efforts. The FEM seems to be a powerful tool in seismic performance verification.

At present, FEM analysis allows some variations with respect to nonlinear soil and RC models. Widely used for academic and design practice purposes are commercial FEM codes that incorporate the representation of skeleton and hysteresis curve between bending moment and curvature of RC beam and pass-dependent hysteresis soil models. An elaborate FEM code that employs fully path-dependent constitutive models of soil and RC has been developed (Shawky and Maekawa 1996). To validate the reliability and accuracy of these nonlinear FEM analyses, numerical analysis correlation studies on experimental data and earthquake damage have been carried out elsewhere. For example, several researchers investigated the failure mechanism of Daikai Station using the nonlinear FEM codes and showed that the analytical results well explained the cause of the failure of the center column of the structure (AN et al. 1997; JSCE 1999; Matsumoto et al. 2003). However, in the case of such case studies, it is naturally impossible to validate the accuracy of time history response associated with such factors as the maximum deformation and interactive earth pressure, during ground motion. Thus, the influence of nonlinear model parameters fluctuation on dynamic response is still unclear.

The scope of this paper is to develop a suitable nonlinear FEM model and validate it based on a large size shake table test that provides the nonlinear response of a RC model associated with dynamic soil-structure interaction. Generally speaking, since the seismic performance of RC members is mostly governed by flexural deformation, we intend to enhance the existing skeleton and hysteresis rules for structural nonlinearity. For this purpose, we first discuss the most favorable rules for establishing the specifications for underground structures such as frame structures having rigid haunch and subjected to earth pressure. Secondly, we present the experimental aspects of inelastic seismic performance of two-box type model RC structures (Ohtomo et al, 2003). Finally, the accuracy of the qualified FEM model is discussed by correlating it with the shake table test results.

[1]Research Engineer, Central Research Institute of Electric Power Industry, Japan
E-mail: j-matsui@criepi.denken.or.jp
[2]Senior Research Engineer, Central Research Institute of Electric Power Industry, Japan
[3]General Maneger, Kansai Elecric Power Co. Ltd., Japan

2. Nonlinear model for RC members

2.1 General

This chapter deals with the qualification of a RC member modeling technique and its verification through correlation with past test data. First, the RC member is modeled as a flexural beam (axial-force dependent trilinear degrading model: the Takeda Model (Takeda et al. 1970). Secondly, we propose a simple reinforcing bar pullout model in the corner region in the skeleton curve of the Okamura-Shima model. Finally, we apply the qualified model to a static load test of RC duct-type structure.

2.2 Modeling of RC members

Several nonlinear models for RC members have already been proposed and widely used in earthquake resistant design. First, nonlinear models of steel structures, such as the bi-linear model and Ramberg-Osgood model, were applied to examine such behaviors as the bending of RC members in terms of the moment-curvature relationship. However, with these models, it is impossible to estimate the deformation performance of an RC member that have exceeded the yielding point in a section and the stiffness of the unloaded member. As is well known, shear and axial forces affect the restoring force and hysteresis characteristics of RC members. Then degrading stiffness models, which have trilinear idealization for the restoring force and simple rules for aspects such as the hysteresis character, were proposed. As a means to estimate a detailed hysteresis nature, the Takeda model (Takeda et al. 1970) was developed based on numerous RC structural experiments, which became the norm in earthquake response analysis.

Thus, the axial force dependent Takeda model shown in **Fig. 1** was employed because underground structure members are affected by fluctuated axial force due to the existence of overburden soil during ground motion. In addition, further improvements were made on the model to more accurately obtain the deterioration of RC member stiffness.

In general, around the footing and corner regions of
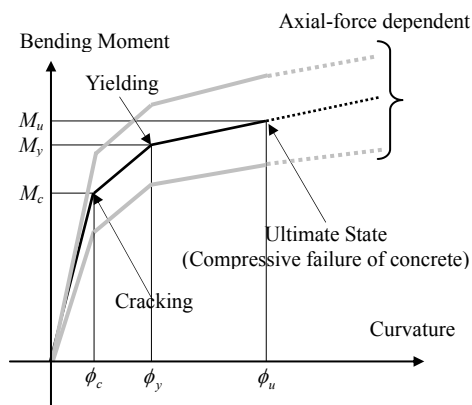
RC members, where the stiffness changes abruptly, reinforcing bar pullout is often observed. This has a major effect on the global load-displacement relationship of the RC structure. Taking this effect into account as simply as possible, many models have been developed. As most of the recent studies on pulling-out of reinforcing bars are based on the local bond stress-local slippage relationship, some procedure to obtain the displacement of reinforcing bar is required. However, the expression in Eq. 1 (Okamura and Maekawa 1991) has the advantage of allowing the estimate of the degree of pullout without using reinforcing bar displacement under a given strain-slippage relationship. With this in mind, we adopted Sima's formulation (Okamura and Maekawa 1991), and proposed a way to apply it to a nonlinear beam element such as a trilinear model.

The slippage between a reinforcing bar and concrete in a corner section is expressed by the following equation.

$$Slip = \varepsilon_s (2 + 3500\varepsilon_s)(f'_c / 20)^{-2/3} D \qquad (1)$$

where *Slip* = slippage due to pull-out, ε_s = strain in reinforcing bar, f'_c = compression strength of concrete, and D = diameter of the reinforcing bar. In order to apply this model to a nonlinear beam element, we develop the following relationship based on **Fig. 2**. The geometric relation in **Fig. 2** may be written as Eq. 2, and rotation angle θ can be transformed as curvature of the beam element in corner regions. Thus we can obtain Eq. 4 by substituting Eq. 2 into Eq. 3,

$$\theta_s = \frac{Slip}{t} \qquad (2)$$

$$\phi_s = \frac{\theta_s}{L} \qquad (3)$$

$$\phi_s = \frac{Slip}{tL} \qquad (4)$$

where ϕ_s = curvature generated by pullout, L = length of discretized beam in corner region, and t = spacing of reinforcing bars.

The position of the second characteristic point (yielding in reinforcement bar) in the restoring force model (trilinear model) is modified by the following equation and can be reflected in the trilinear model as

Fig. 1 Axial-force dependent trilinear model for RC members.
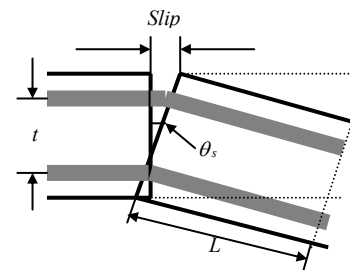
Fig. 2 Modeling of reinforcing bar pull-out.
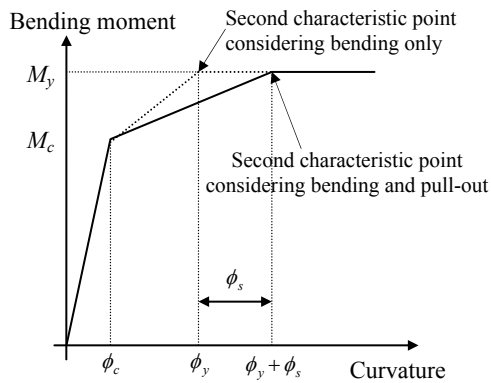
Fig.3 Modification of restoring force model due to pull-out of reinforcing bar.

illustrated in **Fig. 3**.

$$\phi'_y = \phi_y + \phi_s \qquad (5)$$

where ϕ'_y = modified curvature at section of yielding and ϕ_y = original curvature at section of yielding.

2.3 Verification of modeling

To verify the effectiveness of the proposed model as presented in **Fig. 3**, the model was applied to a past static loading test for RC duct-type specimens. **Figure 4** outlines the experiment setup (Honda et al. 1999). The specimen was simultaneously subjected to two types of loading. One loading statically simulated horizontal earthquake loading, which was given from the edge of the top slab, and the other simulated the earth pressure acting on the top slab. Several test cases were performed taking into consideration seismic loading and failure mode aspects as listed in **Table 1**. In this paper, we simulated the basic case, in which the load path was monotonous and the failure mode of specimen was flexural.

Figure 5 illustrates the FEM analysis model used for the basic case. The two box duct-type RC specimen was numerically expressed as nonlinear beam elements, for which the Takeda model, i.e. trilinear model was as-
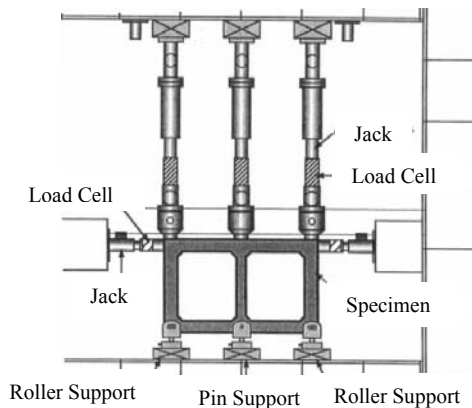
Fig. 4 Loading test setup.

Table 1 Loading test cases.

	Case			
	1	2	3	4
Loading	Monotonous	Cyclic		
Depth of overburden	20 m		5 m	20 m
Failure mode	Bending			Shear
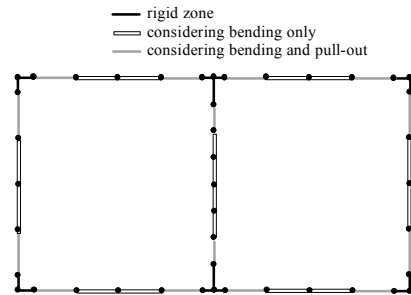
Fig. 5 FEM mesh for analysis of static loading test.

signed. Axial element length was determined as equal to section thickness (200mm) based on the fact that RC member flexural and shear failure zones with respect to member axis stay within the length almost equivalent to the section thickness. To realize rigid haunch behavior at he corner sections, a specified elements having flexural stiffness 1,000 times as high as other beam elements were applied for these parts according to Standard Specifications for Concrete Structures-2002 (Japan Society of Civil Engineering, 2002). The effect of reinforcing bar pullout as presented in Eq. (5) and **Fig. 3** was employed at the elements bordering the corner sections. To characterize the restoring force of the specimen members in trilinear model, three specified points as depicted in **Figs. 2** and **3** are regarded with concrete crack initiation, reinforcement bar yielding and compressive ultimate strain of concrete, respectively. These points are given in the form of moment-curvature relationship developed by a RC section analysis subjected to bending moment and axial force using appropriate RC properties provided by Honda et al. (1999).

To investigate more deeply the effectiveness of the proposed model, two other numerical analysis results were compared with experimental ones as well as the proposed modified Takeda model. Hence, three types of analysis; (a) the traditional Takeda model (Takeda et. al 1970)(See **Fig. 2**), (b) the modified Takeda model (See **Fig.3**) and (c) more sophisticated RC constitutive model (Okamura and Maekawa, 1991) were compared with the experimental results in **Fig. 6**. Note that analytical results with obtained by the model (a) and (b) are presented in this study because the numerical analysis correlation using the model (c) with the experimental re-
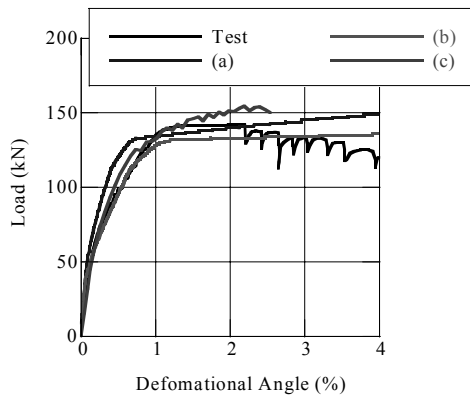
Fig. 6 Result of analysis(test and analysis result was provided by Iizuka et al(1999)).

Fig. 7 Shake table test configuration.

Fig. 8 Model RC Structure.

sults in **Fig. 4** was previously studied (Iizuka et al. 1999).

Figure 6 shows a comparison of experimental and analytical results for the load-relative displacements relationship, using three types of analysis results, as follows. Model (a) is the result by the traditional Takeda model, (b) is by the proposed trilinear model illustrated in **Fig. 3**, and (c) is by the more sophisticated RC constitutive model (Iizuka et al. 1999). Model (a) seems to underestimate the RC structure deformation compared with models (b) and (c). On the other hand, model (b) gives a good estimation for the test result without loss of the threshold of stiffness degradation. In addition, the load-displacement relationships obtained with both (b) and (c) agree well in the region where the deformation angle is less than 1%. This further reinforces the validity of the proposed trilinear model combined with the reinforcement bar pullout model.

3. Shake table test

3.1 General
The shake table test intended for numerical analysis correlation is presented. Some unique test results on dynamic soil-structure interaction and inelastic deformation of the two-box type model RC structure (hereafter, model RC structure) are discussed to facilitate understanding of the following analytical evaluation. Emphasis is placed on the fact that the seismic performance of the model RC structure is totally governed by ground response. Details of the test program and more detailed discussions on the experimental findings were previously reported (Ohtomo et al. 2003).

3.2 Test program
The test was performed in a laminar shear box using a large shake table with a maximum loading capacity of 5000 kN, which is owned by The National Research Institute for Earth Science and Disaster Prevention. The arrangement of the model RC structure in the laminar box is described in **Fig. 7**. The model RC structure was fixed to the base plate of a shake table having an over-

burden depth of 3.0 m. Dry sand with the target relative density of about 87% was used to fill the laminar box. Specific gravity, minimum and maximum void ratio of the sand were 2.69, 0.68 and 1.01, respectively.
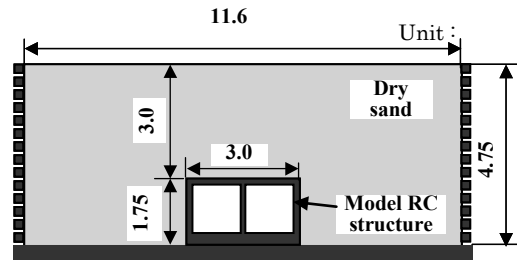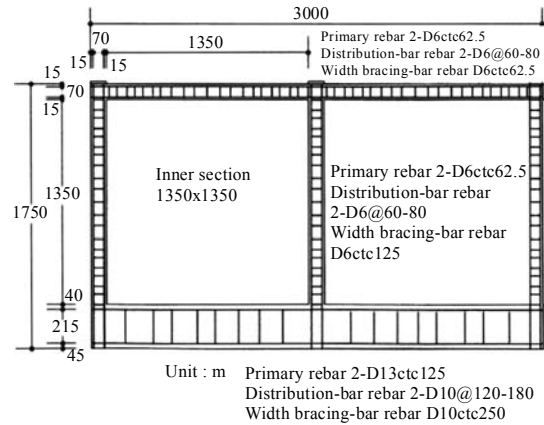
The model RC structure configuration and main reinforcing bar arrangement are illustrated in **Fig. 8**. The inner dimensions of each box were 1.35 m by 1.35 m in one-box inner space, the total outer width was 3.0 m, and the total outer height was 1.75 m. The thickness of the sidewalls and top slab was 0.1 m. The thickness of the bottom slab was 0.3 m. The structural properties of the model RC structures were selected taking into account the fact that the power of the shaking table was such that the models would surely be significantly damaged during excitation. The mechanical properties of the model RC structures are listed in **Table 2**. To facilitate yielding in steel, the main reinforcement D6 was specially treated to lower the yield strength to about 258 N/mm^2.

The apparent shear modulus for the model RC structure whose frame was regarded as a shear deformation element was evaluated at about 8 kN/mm^2. On the other

Table 2 RC properties.

Material	Properties (N/mm^2)	
Concrete	Young's modulus	23500
	Comp. Strength	33.8
	Tensile Strength	2.4
Rebar	Young's modulus	185000
	Yield Strength	265
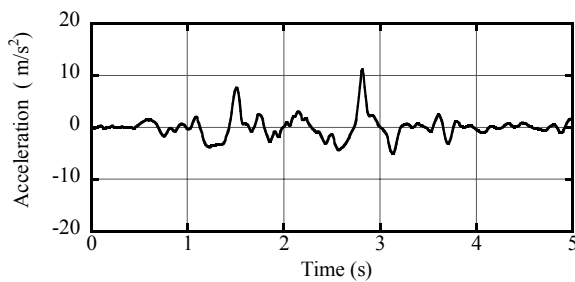
Fig.9 Sample input acceleration.

Fig. 10 Estimated shear stress and strain relationship.

hand, the shear wave velocity was measured at about 180 m/s at the mid-depth of the sand deposit, ranging from 0 m/s to about 200 m/s according to the depth, i.e., from the ground surface to the deposit base. As far as the frame stiffness of the model RC structure is concerned, it accounts for about 20% compared to the surrounding ground. This indicates that the model RC structure sustains excitation in a state of smaller shear stiffness than that of the surrounding ground.

The scaled version of the North-South component of the horizontal ground motion recorded at Kobe University during the 1995 Hyogoken Nanbu Earthquake was employed as the input wave. In fact, the duration was reduced by 50% compared to the observed record so that a predominant period of the observed record was well controlled by the frequency dependent excitation performance of the shake table. Tests were programmed for several different excitation levels with different peak accelerations including 0.6, 1.09, 2.25, 11.27, 4.77, 5.31 and 11.26 m/s^2. **Figure 9** shows the acceleration time history for the 11.27 m/s^2 peak acceleration value.

Measured items and arrangements were developed so as to enable discussion of the model RC structure performance taking account of a number of aspects consisting of acceleration and shear box frame displacement for nonlinear ground response, dynamic earth pressure, shear stress and interface displacement for dynamic soil-structure interaction, and vertical wall transverse displacement relative to the base slab (hereafter, relative displacement), and reinforcing bar and concrete surface strains for inelastic structure deformation.

3.3 Test results and discussion

Representative test results such as interactive shear stress and earth pressure, structural deformation, and concrete cracks development of the model RC structure, were dealt with. Emphasis was placed on the effect of ground deformation on structural performance. Although seven excitations in terms of peak acceleration were carried out, test results under excitation with a peak acceleration of 11.27m/s^2 are discussed for numerical analysis correlation purposes. A significant inelastic structural response actually occurred initially through this specific excitation.

The degree of ground strain induced by excitation with a peak acceleration of 11.27 m/s^2 as shown in **Fig. 9**
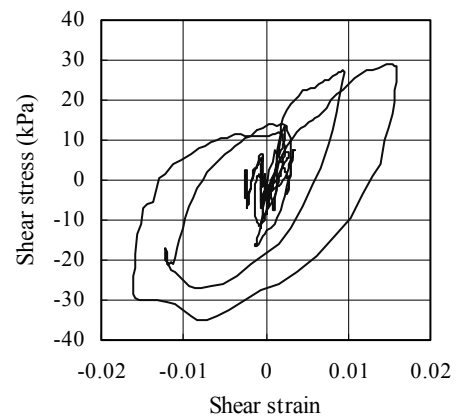
was estimated. The ground strain discussed here was approximately 3.8m in depth. Dynamic shear stress, overburden soil inertia force in other words, was determined using the measured acceleration response. Shear strain was developed based on the relative displacement of the laminar soil box frame.

The stress-strain relationship was then depicted as shown in **Fig. 10**. It can be observed that the maximum shear strain reaches about 1.5%. This indicates a nonlinear ground response; dynamic soil-structure interaction and inelastic deformation during excitation show characteristic correlations under such a large ground strain level.

Dynamic soil-structure interaction and its effect on structural deformation are examined. Time histories of relative ground displacement, shear stress and interface displacement on the upper slab surface of the model RC structure are shown in **Fig. 11**. Response peaks involved in the relative displacement and shear stress time histories are almost identical. This observation indicates that shear stress on the upper slab surface plays a major role on structural deformation. The interface displacement occurs at about 3.0s. At this point in time, the shear stress time history is slightly distorted. However, this response seems to have no effect on the development of relative displacement. These results reflect the condition of the structural stiffness being much smaller than that of the surrounding ground.
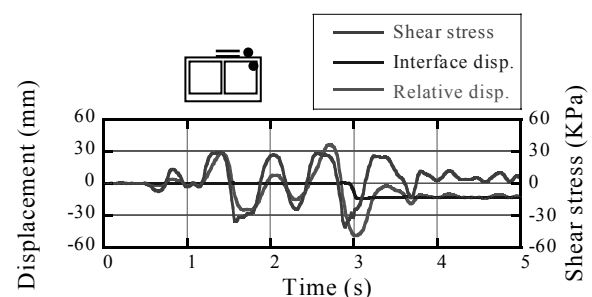
Fig. 11 Time histories of relative displacement, shear stress and interface displacement.
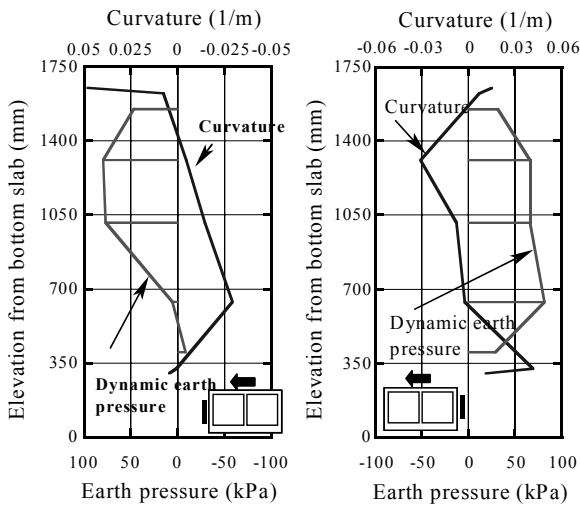
Fig. 12 Dynamic earth pressure distribution at 3.0 s.

Fig. 14 Concrete cracks development on sidewall.

As far as the dynamic earth pressure distribution on the sidewalls is concerned, a unique pattern is clearly observed. **Figure 12** illustrates dynamic earth pressure distributions and curvatures of both sidewalls at approximately 3.0s. Although the model RC structure bears shear deformation as discussed previously, the dynamic earth pressures act in a compressive manner for both sidewalls, with a peak value at the mid height of the sidewall. In addition, the curvature distribution implies that deformation accompanied by inward deflection of the sidewalls occurred at this time.

The correlation between the relative displacement and the ground deformation is also examined. The time histories of the relative and ground displacements are superimposed in **Fig. 13**. The relative displacement is almost identical with the ground displacement. As we presented in an earlier paper (Ohtomo et al. 2003), the relative yielding displacement, i.e. the relative displacement at which the first reinforcement bar yielding occurs, is about 4 mm, while the maximum relative displacement accounts for about 50 mm; therefore, the ratio of maximum to yielding displacement is estimated as 12 to 13. In addition, this observation demonstrates that the relative displacement is fully governed by the ground deformation in the elastic to inelastic ranges. This pattern is also strongly affected by the smaller shear stiffness ratio of the model RC structure to the surrounding ground.

Significant concrete cracks were identified after a se-

ries of shake table tests. **Figure 14** shows cracks on the outer and inner surface of one of the sidewalls. Bending cracks formed at the upper and lower corners. This demonstrates flexural type deformation of the model RC structure. On the contrary, a number of flexural cracks exist along reinforcing bar spacing on the inner wall. These cracks are undoubtedly a reflection of tension stress condition on the inner sidewall face and inward deflection. A unique dynamic earth pressure as discussed in **Fig. 12** definitely caused such crack development.

4. Numerical analysis correlation

4.1 General
This chapter deals with a numerical analysis correlation with the shake table test discussed in chapter 3 to validate the proposed model. Here, a soil-structure interaction model incorporated with the nonlinear RC member model is developed and a dynamic response analysis is performed. Then, the accuracy of the numerical analysis in terms of dynamic ground response, soil-structure interaction and the structural deformation respectively is examined.

4.2 Analysis conditions
Two-dimensional FEM meshes for the analysis were developed taking into account the size of the laminar shear box as sketched in **Fig. 15(a)**. The RC model was also dealt with FEM model (See **Fig. 15(b)**) followed by the similar manner as explained in **Section 2.3**. A horizontal roller condition was assigned for the side boundary condition with a mass that represented the effect of the inertia force caused by the frame of the laminar shear box. The prescribed nodal condition was used for the bottom boundary. The soil nonlinearity was modeled using the Ramberg-Osgood model (hereafter, R-O model), which is a total stress and hysteresis dependent model. The axial force dependent Takeda model with reinforcement bar pullout as presented in **Fig. 3** was used for the model RC structure. Since slippage between the soil and structure was observed in the shake table test as shown in **Fig. 11**, an appropriate slippage

Fig. 13 Time histories of relative displacement.

Number of Elements : 760, Number of Nodes : 837

→ Soil

RC Model

(a) Global model

(b) RC Structure
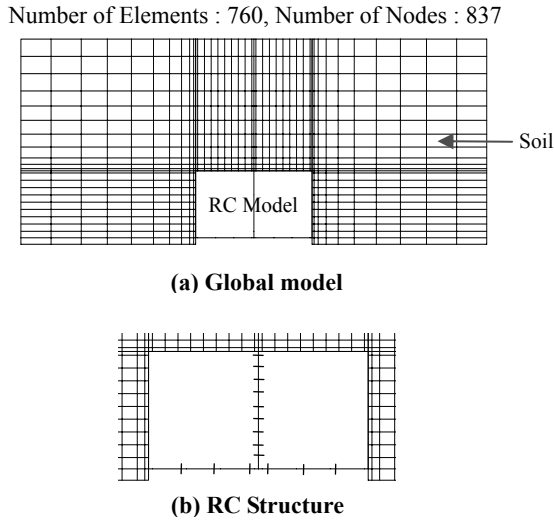
Fig.15 Finite Element Mesh for Shake table test.

and separation model, i.e. a joint element was used. The dynamic response analysis was conducted by using the time history of acceleration response measured at the base of the laminar shear box (as shown in **Fig. 9**; maximum acceleration value = 11.27m/s^2).

To express the nonlinearity of soil, the R-O model was adopted in view of matching complexity with the RC model used in the following manner.

$$\gamma = \frac{S_u}{G_0} s \left(1 + \alpha |s|^{\beta}\right) \tag{6}$$

where s = normalized shear stress ($= \tau / S_u$), γ = shear stress, G_0 = initial shear modulus, S_u = shear strength, α = coefficient depending γ_f, β = parameter for specifying the shape of the skeleton curve. Initial shear modulus of sand (G_0) was obtained from the following expression using measured V_s and ρ in the laminar shear box.

$$G_0 = \rho V_s^2 \tag{7}$$

where V_s and ρ are the shear wave velocity and mass density of the sand, respectively.

Coefficient α (Ohsaki et al. 1978) in Eq. 6 is determined in the following manner. In the R-O model, it is difficult to estimate the reduction in shear stiffness of the soil in the whole shear strain range while maintaining a consistent accuracy. Therefore, we paid attention to the larger shear strain of the soil such as 3%, which was measured in the shake table test as shown in **Fig. 10**, and defined it as the strain at failure (γ_f). The shear stress corresponding to that strain was derived from the result of element tests on soil (Kawai et al. 2003). Reference strain (γ_r) and coefficient α were calculated according to Eqs. 8 and 9, respectively.
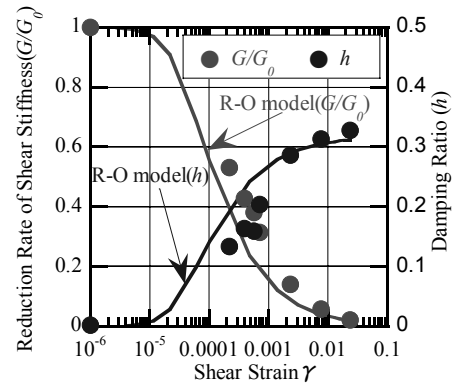
Fig. 16 Dynamic properties and R-O model for siliceous sand No. 5.

$$\gamma_r = \frac{\tau_f}{G_0} \tag{8}$$

$$\alpha = \frac{\gamma_f}{S_u / G_0} - 1 \tag{9}$$

coefficient β was also determined from the regression analysis for the test data of damping ration of sand in Eq. 10.

$$h = \left(\frac{2}{\pi}\right)\left(\frac{\beta}{\beta + 2}\right)\left(1 - \frac{G}{G_0}\right) \tag{10}$$

where h = damping ratio of soil. To define the hysteresis loop, we applied Masing's Rule (Masing 1926) as it is widely used in design practice. An R-O model fitting with experimental results is depicted in **Fig. 16** for the case of mean effective stress of 20kPa.

Restoring force characteristics that express the relationships between bending moment and curvature for RC members were modeled using an axial force dependent trilinear degrading model. Here, three characteristic points corresponded to crack initiation; the yielding of reinforcement bar and the compressive failure of concrete. These values were calculated by section analysis subjected to simultaneous axial force using the RC properties listed in **Table 2**. To ensure axial force dependent nature, the above mentioned three characteristics points are re-assigned in accordance with moment-axial force interaction curves resulting from dynamic axial force. The intact curves are developed by preliminary dynamic analysis using liner properties with respect to soils and RC members. Hysteresis rule is described as unloading stiffness K_d and given by

$$K_d = \frac{M_c}{\phi_c} \left|\frac{\phi_{max}}{\phi_c}\right|^A \tag{11}$$

where ϕ_c = moment at crack initiation, ϕ_{max} = maximum response curvature and A = coefficient of unloading stiffness. Coefficient A is determined as equal to
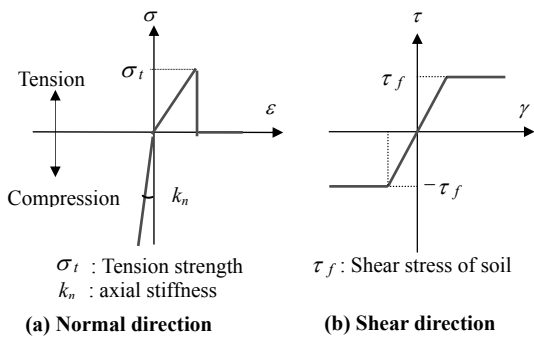
Fig. 17 Constitutive relationship of joint element.

–0.5 as it is widely used in design practice and academic works.

To express slippage and separation between soil and structure, joint elements were assigned to the interface of the model illustrated in **Fig. 17**. In the joint model used here, slippage is supposed to occur when dynamic shear stress exceeds the shear strength of sand (τ_f), while separation is defined to occur when dynamic normal stress reaches initial earth pressure. In addition, separation occurrence indicates slippage as well. To estimate shear strength, the Mohr-Coulomb law was used as shown in Eq. 12.

$$\tau = c - \sigma \tan \theta \qquad (12)$$

where c = cohesion and θ = friction angle. c and θ were originally determined as 0 kPa and 35 degrees corresponding to the sand used in the shake table test, respectively. To represent less friction performance between sand and concrete, the estimated θ =35 degrees was further lowered by multiplication by 2/3 in accordance with one of the current foundation design specifications (Japan Road Association 2002).

4.3 Results and discussion

Numerical analysis correlation is presented in terms of nonlinear ground response, dynamic soil-structure interaction and inelastic structural deformation. Most of related test results dealt with here are discussed in the preceding chapter. Validation of the analysis focused on nonlinear model parameter identification and its effect on the analysis result.

Ground response was first examined in terms of displacement and acceleration. **Figure 18** compares the test and analytical results for the vertical distributions of maximum horizontal displacement and acceleration, respectively. As we can clearly see in **Fig. 18(b)**, the analytical results for displacement response agree well with the test results. On the other hand, some degree of discrepancy between test and analysis results is observed in the shallower part. This is probably due to an inaccurate representation of soil nonlinearity under such a low confining pressure. As far as acceleration response is concerned, the analysis results adequately explain the degradation of acceleration amplitude with

(a) accerelation   (b) displacement
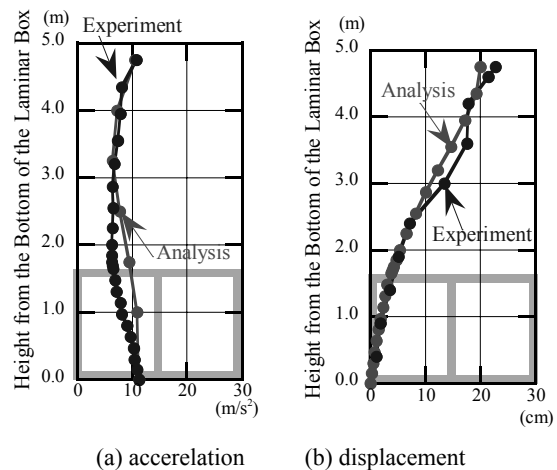
Fig. 18 Distribution of maximum value of horizontal ground response.

respect to depth arising from strong soil nonlinearity in **Fig. 18**. From the judgment that the analytical results give a good estimation for ground response as seen in **Fig. 18**, the model parameter characterization in the R-O model is considered to be successfully determined using the laboratory soil test data.

Computed relative displacement of the model RC structure is compared with the test result in **Fig. 19**. The analytical results on time history harmonizes well not only with peaks but also with phase trace involved in the test results. The analytical results also show that the surrounding ground controls the maximum sidewall deformation, as observed in the test results.

As discussed previously, the model RC structure performance is largely controlled by the surrounding ground displacement in **Fig. 20**. In this respect, the accuracy of the analytical results seems to be largely dependent on a successful modeling of soil nonlinearity. RC members naturally deform in accordance with ground deformation.

The effect of dynamic soil-structure interaction is then analytically examined. As we observed in **Fig. 11**, the shear stress on the upper slab surface played an important role on structural deformation. Based on this finding, the interface performance in terms of shear stress and the interface displacement is discussed. **Fig-**
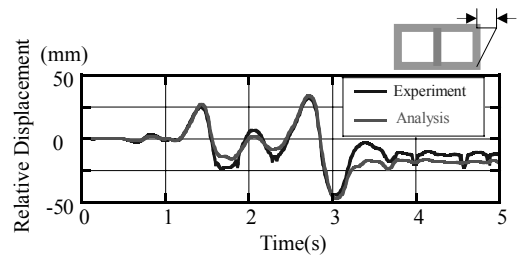
Fig. 19 Time histories of relative displacement between top and bottom slabs.
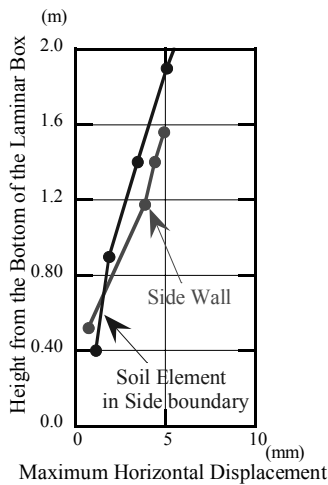
Fig. 20 Comparison maximum horizontal displacement between sidewall of specimen and side boundary element of soil.
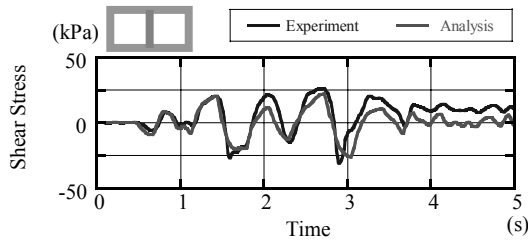
Fig. 21 Time histories of shear stress acting on top slab.
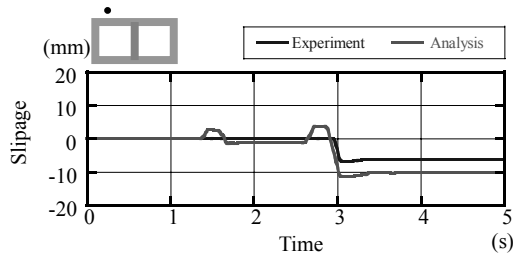
Fig. 22 Time histories of relative displacement between soil and top slabs of specimen.

ure 21 presents the time histories of shear stress based on both test and analytical results. The analytical results provide a good estimation for the shear stress response, particularly between 0 s and 3.0 s, the duration in which a substantial structural response occurs. This fact may be the cause of the good estimation for the relative displacement. **Figure 22** shows the analytical estimation for the interface displacement. The interface displacement is evaluated as the sum of axial strain in elements allocated along the top slab face in the analysis model. Although the magnitude of interface displacement involves some uncertainties, evaluation of displacement increase is considered essential. In this respect, the analytical result provides a satisfactory estimation at 3.0 s in which the interface displacement is clearly observed.

This appears to be the result of the appropriate assignment of internal friction angle along the concrete surface, at least under the test condition covered in this paper.

Next, the accuracy of analysis is discussed with regard to inelastic structural deformation. In this study, as flexural type nonlinearity is idealized using the trilinear model as presented previously, the first and second characteristics points become responsible for structural nonlinearity. As the first characteristics point is defined as concrete crack development, **Fig. 23** compares the crack distributions in the model RC structure section obtained from the test with analytical results. Here, the test results are shown as a sectional view version of **Fig. 14**. On the other hand, the computed bending moments at the respective beam element of the model RC structure are checked for whether or not they exceed the specific bending moment in the trilinear moment and curvature relationship. Positive and negative moment values are considered and appropriately assigned to the outer and inner sides of the RC member. As clearly seen

(a) Test

■ : rigid zone
■ : occurrence of crack
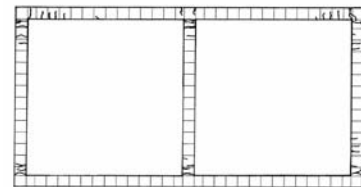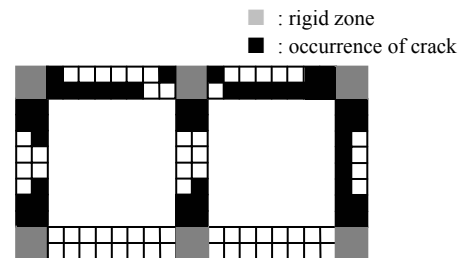
(b) Analysis

Fig. 23 Comparison of final crack distribution.

in **Fig. 23**, the crack development patterns are almost identical between the test and analytical results, and
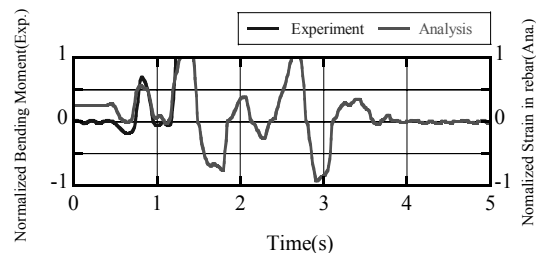
Fig. 24 Time histories of steel strain (test) and moment (analysis) as measure for judgment of yielding.

Table 3 Evaluation of indices for verification of seismic performance.

Index			Test	Analysis
Displacement in Rebar Yield	δ_y	(mm)	3.9	6.7
Maximum Displacement	δ_{max}	(mm)	43.8	46.1
Ductility Factor	δ_{max}/δ_y	-	11.2	6.9
Deformation Angle	δ_{max}/H	(%)	3.6	3.4

penetration cracks at corners are particularly well evaluated.

For the validation of second characteristics point, the normalized reinforcement bar strain and structural member moment obtained from the test and analytical results are examined. The vertical axis on the right hand in **Fig. 24** presents reinforcing bar strain normalized by the yielding strain. The left hand vertical axis represents measured moment normalized by yielding moment that is defined as the second specified point in the trilinear characterization of the nonlinear RC model. Thus it becomes possible to indirectly compare the threshold of inelastic response. It is possible to identify the increase of these yielding indices occurring almost the same instant at the lower corner. Moreover, a similar evaluation shows that the yielding events at the corners of model RC structure are effectively identified using the trilinear model. These findings indicate that the flexural nonlinear model using the tri-linear model is valid.

To examine the accuracy of the qualified FEM model discussed in this paper, some indices that may express the degree of flexural type structural deformation are introduced. These are yielding relative displacement, maximum relative displacement, ductility factor (the ratio of the maximum relative displacement to the yielding relative displacement) and deformation angle (normalized relative displacement with respect to the model RC structure height). **Table 3** shows the values of these indices obtained from the test and analytical results. As mentioned earlier, the parameters for the R-O model were determined based on the maximum strain level in soil found in the test. This might have led to a substantial overestimate of displacement at the time of initial yielding. In other words, the analytical model applied here seems to be more suited for the post-yielding range. Under the specific test condition here, the maximum relative displacements or deformation angles are considered more reasonable than ductility factors normally employed for the seismic performance evaluation of above-ground structures.

5. Conclusions

Large shake table test and subsequent analysis correlation were conducted to develop and validate a suitable nonlinear FEM model for the seismic performance of underground structures, enhancing existing skeleton and hysteresis rules for RC members. The main conclusions obtained through this study are summarized as follows.

(1) A nonlinear RC member model was qualified on the basis of axial force dependent trilinear model. To represent stiffness degradation more accurately, we incorporated the effect of reinforcement bar pullout with the existing trilinear model. As a result, an advanced version of the trilinear model that provides the extended second characteristics point in flexural moment and curvature relationship was presented. The validity of the proposed model was then examined through numerical correlation analysis using a past static load test for a box-type RC structure. The analytical results were found to have a good correlation with test data as well as other numerical analytical results based on RC constitutive law based-nonlinear analysis.

(2) Some unique aspects of the model RC structure performance were presented. The degree of ground strain induced by an excitation with peak acceleration of 11.27 m/s^2 was estimated as about 1.5%. Under this excitation condition, dynamic shear stress on the upper slab surface plays a major role on structural deformation. In addition, the relative displacement was fully governed by the ground deformation both in the elastic and inelastic ranges. These global shear deformation natures were considered to be as a result of the smaller shear stiffness ratio of the model RC structure to the surrounding ground. As an evidence of inelastic shear deformation, bending cracks penetrated at the upper and lower corners of the sidewalls. While a number of flexural cracks developed at the central portion on the inner wall. These crack patterns were undoubtedly a reflection of unique dynamic earth pressure in which the earth pressure acts in a compressive manner for both sidewalls.

(3) The FEM model developed in this paper derives estimation that showed good correlation with test results in terms of such factors as relative displacement, shear stress on the upper slab surface crack patterns and reinforcement bar yielding events. Since the performance of the model RC structure was largely dependent on the deformation of surrounding ground, the appropriate nonlinear modeling of soil and the subsequent estimation of ground response resulted in a reasonable estimation of structural performance. As long as flexural type deformation was concerned, trilinear representation of RC members was found to be valid particularly in assessing the inelastic structural deformation. For the purpose of seismic performance verification for underground structures, the numerical correlation analysis extended to represent the relevant deformation representation indices such as the deformation angle and maximum relative displacement instead of ductile factor.

References

An, X., Shawky, A. and Maekawa, K. (1997). "The collapse mechanism of a subway station during the Grate Hanshin Earthquake." *Cement and Concrete Composites*. 19, 241-257.

Editorial committee for the report on the Hanshin-Awaji earthquake disaster, JSCE (1999) "Report on the Hanshin-Awaji earthquake disaster -Investigation of cause of damage to civil engineering structures-." (in Japanese), 304-309.

Honda, K., Adachi, M., Ishikawa, H. and Hasegawa, T. (1999). "Experimental study on deformation property of box culvert subjected to lateral load." *Proceedings of the Japan Concrete Institute*, 21 (3), 1261-1266. (in Japanese).

Iida, H., Hiroto, T., Yoshida, N. and Masahiko, I. (1996). "Damage to Daikai subway station." *Special Issue of Soils and Foundations,* 283-300.

Iizuka, K., Adachi, M., Honda, K. and Takeda, T. (1999). "Analytical study of nonlinear behavior of box culvert by FEM." *Proceedings of the Japan Concrete Institute*, 21 (3), 1267-1272. (in Japanese).

Japan Society of Civil Engineers (2002). "Standard specifications for concrete structures-2002, Structural performance verification." (in Japanese).

Japan Road Association (2002). "Reference for highway bridge design specifications for highway bridges part VI; Substructures."

Kawai, T., Kanatani, M., Ohtomo, K., Matsui, J. and Matsuo, T. (2003). "Development of advanced earthquake resistance performance verification on reinforced concrete underground structure Part 2 -Verification of the ground modeling methods applied to non-linear soil-structure interaction analysis-." *CRIEPI Report* U02018. (in Japanese).

Masing, G. "Eigenspannungen und Verfestigung beim Messing." (1926). *Proceedings of 2nd International Congress of Applied Mechanics*, 332-335.

Matsui, J., Kanazu, T. and Endoh, T. (2002). "Proposal of a practical nonlinear model used for seismic performance verification of reinforced concrete underground structures." *CRIEPI Report* U01041. (in Japanese).

Matsumoto, T., Ohtomo, K., Irie, M. and Ikezawa, I. (2003). "Study on causes of seismic damage to in-ground RC structures with highly compressed column." CD-ROM *Proc. of the Japan Concrete Institute*, 25, 1579-1584. (in Japanese).

Ohsaki, Y., Hara, T. and Kiyoda, S. (1978). "A Proposal on a dynamic soil model for excitation analysis and an example of its application." *Proceedings of 5th Earthquake Engineering Symposium*, 697-704. (in Japanese).

Ohtomo, K., Suehiro, T., Kawai, T. and Kanaya, K. (2003). "Substantial cross section plastic deformation of underground reinforced concrete structures during strong earthquake." *Proc. of JSCE* 724 (I-62), 157-174. (in Japanese)

Okamura, H. and Maekawa, K. (1991). "*Non-linear analysis and constitutive laws for reinforced concrete structures.*" Gihoudo Publishing Co., Ltd.

Shawky, A. and Maekawa, K. (1996). "Computational approach to path-dependent nonlinear RC/soil interaction." *Proc. of JSCE* 532 (V-30), 197-207.

Takeda, T., Sozen, M. A. and Nilsen, N. N. (1970) "Reinforced concrete response to simulate earthquake." *Journal of Structural Division, ASCE*, 96 (2), .ST12, 2557-2573.